Ruthenium-Nitrosyl Complexes with Glycine, L-Alanine, L-Valine, L-Proline, D-Proline, L-Serine, L-Threonine and L-Tyrosine: Synthesis, X-ray Diffraction Structures, Spectroscopic and Electrochemical Properties and Antiproliferative Activity

Anna Rathgeb,[#] Andreas Böhm,[#] Maria S. Novak,[#] Anatolie Gavriluta,[‡] Orsolya Dömötör,[†] Jean Bernard Tommasino,[‡] Éva A. Enyedy,[†] Sergiu Shova,[§] Samuel Meier,[#] Michael A. Jakupec,[#] Dominique Luneau,*[,‡] Vladimir B. Arion*[,#]

[#]*University of Vienna, Institute of Inorganic Chemistry, Währinger Strasse 42, A-1090 Vienna, Austria*

[‡]*Université Claude Bernard Lyon 1, Laboratoire des Multimatériaux et Interfaces (UMR 5615), Campus de La Doua, 69622 Villeurbanne Cedex, France*

[†] *Department of Inorganic and Analytical Chemistry, University of Szeged, Dóm tér 7. H-6720 Szeged, Hungary*

[§] *"Petru Poni" Institute of Macromolecular Chemistry of the Roumanian Academy, Aleea Grigore Ghica Vodă 41-A, RO-700487 Iasi, Romania*

Abstract

The reactions of $[Ru(NO)Cl_5]^{2-}$ with glycine (Gly), L-alanine (L-Ala), L-valine (L-Val), L-proline (L-Pro), D-proline (D-Pro), L-serine (L-Ser), L-threonine (L-Thr), and L-tyrosine (L-Tyr) in *n*-butanol or *n*-propanol afforded eight novel complexes of the general formula $[RuCl_3(AA{-}H)(NO)]^{-}$, where AA = Gly, L-Ala, L-Val, L-Pro, D-Pro, L-Ser, L-Thr, L-Ser and L-Tyr, respectively. The compounds were characterized by elemental analysis, electrospray ionization mass spectrometry (ESI-MS), ^{1}H NMR, UV−vis, ATR IR spectroscopy, cyclic voltammetry and X-ray crystallography. X-ray crystallography studies have revealed that in all cases the same isomer type (from three theoretically possible), has been isolated, namely *mer*(Cl), *trans*(NO,O)-$[RuCl_3(AA{-}H)(NO)]$, as it was also recently reported for osmium analogs with Gly, L-Pro and D-Pro (see *Z. Anorg. Allg. Chem.* **2013**, *639*, 1590−1597). Compounds **1**, **4**, **5** and **8** were investigated with regard to their stability in aqueous solution and reactivity towards sodium ascorbate by ESI-MS. In addition, cell culture experiments in three human cancer cell lines, namely A549 (nonsmall cell lung carcinoma), CH1 (ovarian carcinoma) and SW480 (colon adenocarcinoma) have been performed and the results discussed in conjunction with the lipophilicity of compounds.

Keywords: Ruthenium, Nitrosyl, Amino acids, Antitumor activity

Introduction

Nitric oxide plays important roles in biochemical processes,[1] and, in particular, in progression of human tumors.[2] The antimetastatic activity of NAMI-A, an investigational drug in phase II clinical trials,[3] was suggested to be related to its interaction with NO *in vivo*.[4] Given the importance of NO as a noninnocent ligand in coordination chemistry,[5] the occurrence of structural trans effects (STEs), the role of the metal-nitrosyl unit as a reaction mediator or regulator of geometry around the metal ion,[6] as well as linkage isomerization of the N- and O-bound nitrosyl ligand,[7] surprisingly little is known about the reactivity of ruthenium(II)- and osmium(II)-nitrosyl compounds with respect to amino acids. Although a few ruthenium-nitrosyl complexes with amino acids and related ligands have been reported in the literature, e.g., $K[Ru(Gly)(OH)_3NO]$,[8] $K[Ru(L\text{-}Ala)(OH)_3NO]$,[9] $[RuCl_2(L\text{-}His)(NO)]$,[10] $[RuCl_2(L\text{-}Met)(NO)]$[11] and $(C_2H_5)_4N[RuCl_3(pyca)(NO)]$,[12] where pycaH = 2-pyridinecarboxylic acid, their antiproliferative activity remains unknown. All this prompted us to continue our recently initiated study[13] on the interaction of $[MCl_5(NO)]^{2-}$ with different amino acids as a benchmark for further investigation of the reactivity of ruthenium and osmium nitrosyl complexes with azole heterocycles towards amino acids (AA).

Moreover, we reported recently on the synthesis of two series of transition metal complexes, namely (cation)[cis-MCl_4(Hazole)(NO)] and (cation)[*trans*-MCl_4(Hazole)(NO)], where M = Ru, Os and Hazole = 1*H*-indazole, 1*H*-pyrazole, 1*H*-imidazole or 1*H*-benzimidazole. Ruthenium and osmium analogs showed a striking difference in antiproliferative activity in three human cancer cell lines A549 (nonsmall cell lung carcinoma), CH1 (ovarian carcinoma) and SW480 (colon adenocarcinoma).[14,15] These results were in strong contrast to previous comparative studies on homologous ruthenium and osmium complexes (with metal ion in different oxidation states) showing either similar activities[16,17] or much smaller differences[18,19,20] than those observed for compounds reported in ref. 15. We are now trying to find out whether their behavior towards amino acids can provide an explanation for their different antiproliferative activity. Amino acids are the basic units of proteins and the most important low-molecular-weight biological ligands. They are major ingredients of the media used in cell culture experiments.[21] In

addition, reactions with amino acids are likely to be involved in speciation of metal complexes during biotransformation in the body. Knowledge about these reactions will therefore help in elucidating the species delivered into the cell and in better understanding the mechanisms of drug metabolisation or detoxification.[22] For example, a [(Pt(L-Met)$_2$] species was isolated from the urine of cancer patients treated with cisplatin. This is one of the few known metabolites of the drug.[23]

Chart 1

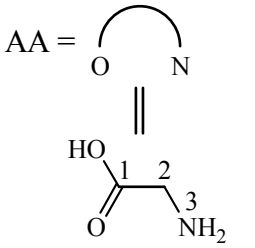

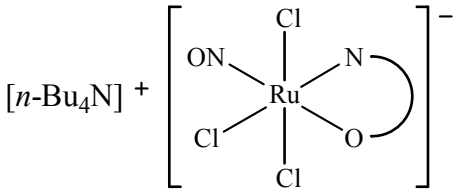

[*n*-Bu$_4$N][RuCl$_3$(AA-H)(NO)]

Glycine (Gly)

L-Alanine (L-Ala)

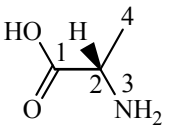

L-Valine (L-Val)

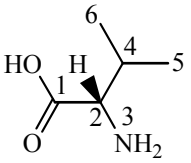

L-Proline (L-Pro)

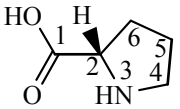

D-Proline (D-Pro)

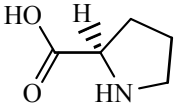

L-Serine (L-Ser)

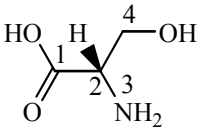

L-Threonine (L-Thr)

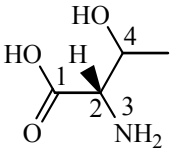

L-Tyrosine (L-Tyr)

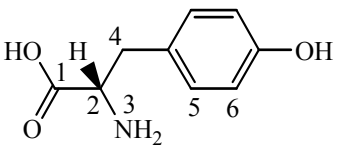

AA	**Complex**
Gly	**1**
L-Ala	**2**
L-Val	**3**
L-Pro	**4**
D-Pro	**5**
L-Ser	**6**
L-Thr	**7**
L-Tyr	**8**

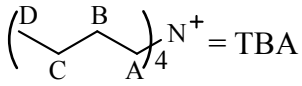

Herein we report on the synthesis of eight new ruthenium(II)-nitrosyl complexes with Gly, L-Ala, L-Val, L-Pro, D-Pro, L-Ser, L-Thr and L-Tyr (Chart 1), their X-ray

diffraction structures, spectroscopic and electrochemical properties, lipophilicity, behavior in aqueous solution and antiproliferative activity in human cancer cell lines *in vitro*. The latter was compared to that of osmium-nitrosyl complexes with Gly (**1***), L-Pro (**4***) and D-Pro (**5***).

Experimental Section

Materials. The starting compounds $Na_2[RuCl_5NO]\cdot 6H_2O$ and $(n Bu_4N)_2[RuCl_5NO]$ were synthesized as previously reported in the literature.[24] $RuCl_3\cdot H_2O$ was purchased from Johnson Matthey, sodium nitrite (97%), tetrabutylammonium chloride (97%), L-Thr, L-Ala and Gly (99%) were from Sigma-Aldrich. L-Ser was from Serva, L-Pro (99%) and D-Pro (99%) were from Alfa Aesar and L-Tyr (99%), formic acid and sodium ascorbate were from Fluka. All chemicals were used without further purification. Methanol (HPLC grade, Fisher) and ultra-pure water (18.2 MΩ, Advantage A10, 185 Ultrapure Water System, Millipore, France) were used for ESI-MS study.

Synthesis of Complexes

($n Bu_4N$)[$RuCl_3$(Gly−H)(NO)] (1). A mixture of $Na_2[RuCl_5NO]\cdot 6H_2O$ (400 mg, 0.86 mmol), $n Bu_4NCl$ (362 mg, 1.31 mmol) and Gly (121 mg, 1.61 mmol) was refluxed in *n*-butanol (10 mL) for 1.5 h. The solution was allowed to cool to room temperature. The separated salt was filtered off. The solution was transferred into a beaker. Dark red crystals formed after several days were filtered off and washed with water/ethanol 1:3 (4 mL), diethyl ether (4 mL) and dried *in vacuo*. Yield: 75 mg, 15.5%. Anal. Calcd for $C_{18}H_{40}Cl_3N_3O_3Ru$ (M = 553.96 g/mol): C, 39.03; H, 7.28; N, 7.59. Found: C, 38.77; H, 6.96; N, 7.43. ESI-MS in MeOH (negative): ESI-MS in MeOH (negative): *m/z* 312.72 $[RuCl_3NO(Gly - H)]^-$ (m_{theor} = 312.83), 274.70 $[RuCl_2NO(Gly - 2H)]^-$ (m_{theor} = 274.86), 238.71 $[RuClNO(Gly - 3H)]^-$ (m_{theor} = 238.88). IR, cm^{-1}: 886, 1160, 1301, 1490, 1669 (vs) $\nu_{as}(COO^-)$, 1862 (vs) ν(NO), 2955 (m) ν(CH), 3124 (m) $\nu_s(NH_2)$ and 3193 (m) $\nu_{as}(NH_2)$. UV−vis (buffer), λ_{max}, nm (ε, $M^{-1}cm^{-1}$): 279 (1790), 453 (104). ^{1}H NMR (500.32 MHz, DMSO-d_6): δ 0.95 (t, $12H_D$, J = 7.5 Hz), 1.32 (sxt, $8H_C$, J = 7.3 Hz), 1.58 (qui, $8H_B$, J = 7.8 Hz), 3.17 (m, $8H_A$, J = 8.2 Hz), 3.36 (t, J = 6.5 Hz, 2H, H_2), 5.89 (s, 2H, H_3) ppm. For assignment of proton resonances see atom numbering in Chart 1.

(nBu$_4$N)[RuCl$_3$(L-Ala–H)(NO)] (2). A mixture of $Na_2[RuCl_5NO]\cdot 6H_2O$ (400 mg, 0.86 mmol), nBu$_4$NCl (450 mg, 1.62 mmol) and L-Ala (115 mg, 1.29 mmol) was refluxed in *n*-butanol (10 mL) for 1.5 h. The solvent was removed under reduced pressure and the remaining oil was dried *in vacuo*. Water (7 mL) was added. The solution was decanted into a beaker and allowed to stand at room temperature. Five days later orange crystals were filtered off and a second fraction was collected two days later. The product was washed with water/ethanol 1:1 (4 mL), diethyl ether (4 mL) and dried *in vacuo*. Yield: 102 mg, 21.0%. Anal. Calcd for $C_{19}H_{42}Cl_3N_3O_3Ru$ (M = 567.98 g/mol): C, 40.18; H, 7.45; N, 7.40. Found: C, 40.15; H, 7.72; N, 7.05. ESI-MS in MeOH (negative): *m/z* 326.69 $[RuCl_3NO(L\text{-Ala} - H)]^-$ (m_{theor} = 326.85), 288.68 $[RuCl_2NO(L\text{-Ala} - 2H)]^-$ (m_{theor} = 288.87), 252.68 $[RuClNO(L\text{-Ala} - 3H)]^-$ (m_{theor} = 252.89). IR, cm^{-1}: 873, 1181, 1266, 1224, 1470, 1577, 1666 (vs) $\nu_{as}(COO^-)$, 1858 (vs) ν(NO), 2874, 2960 ν(CH), 3120 (m) $\nu_s(NH_2)$ and 3190 (m) $\nu_{as}(NH_2)$. UV−vis (buffer), λ_{max}, nm (ε, $M^{-1}cm^{-1}$): 279 (1857), 453 (104). ^{1}H NMR (500.32 MHz, DMSO-d_6): δ 0.95 (t, 12H$_D$, J = 7.4 Hz), 1.32 (m, 12H, 8H$_C$, 3H$_4$), 1.58 (qui, 8H$_B$, J = 7.8 Hz), 3.17 (t, 8H$_A$ J = 8.2 Hz), 3.59 (qua, 1H, H$_2$, J = 7.3 Hz), 5.28 (m, 1H, H$_{3'}$) and 6.39 (m, 1H, H$_{3''}$) ppm.

(nBu$_4$N)[RuCl$_3$(L-Val–H)(NO)] (3). A mixture of $Na_2[RuCl_5NO]\cdot 6H_2O$ (400 mg, 0.86 mmol), nBu$_4$NCl (450 mg, 1.62 mmol) and L-Val (151 mg, 1.29 mmol) was refluxed in *n*-butanol (10 mL) for 2 h. The solvent was removed under reduced pressure and the remaining oil was dried *in vacuo*. Water (7 mL) was added. The solution was decanted into a beaker and allowed to stand at room temperature. Seven days later orange crystals formed were filtered off, washed with water/ethanol 1:1 (4 mL), diethyl ether (4 mL) and dried *in vacuo*. Yield: 179 mg, 35.0%. Anal. Calcd for $C_{21}H_{46}Cl_3N_3O_3Ru\cdot 0.5H_2O$ (M = 605.05 g/mol): C, 41.69; H, 7.83; N, 6.94. Found: C, 41.69; H, 8.14; N, 6.73. ESI-MS in MeOH (negative): *m/z* 355 $[RuCl_3NO(L\text{-Val} - H)]^-$ (m_{theor} = 354.88), 317 $[RuCl_2NO(L\text{-Val}-2H)]^-$, 281 $[RuClNO(L\text{-Val}-3H]^-$. IR, cm^{-1}: 806, 894, 1012, 1180, 1299, 1372, 1467, 1663 (vs) $\nu_{as}(COO^-)$, 1852 (vs) ν(NO), 2878, 2962 (m) ν(CH) and 3187 (m) $\nu(NH_2)$. UV−vis (buffer), λ_{max}, nm (ε, $M^{-1}cm^{-1}$): 279 (1883), 453 (104). ^{1}H NMR (500.32 MHz, DMSO-d_6): δ 0.86 (d, 3H, H$_6$, J = 7.9 Hz), 0.95 (t, 12H$_D$, J = 7.4 Hz), 0.99 (d, 3H, H$_5$ J = 7.9), 1.32 (sxt, 8H$_C$, J = 7.4 Hz),

1.58 (qui, 8H_B, J = 7.8 Hz),2.19 (m, 1H, H_4), 3.17 (t, 8H_A J = 8.2 Hz), 3.44 (m, 1H, H_2), 4.67 (m, 1H, $H_{3'}$), 6.44 (m, 1H, $H_{3''}$) ppm.

(*n*Bu$_4$N)[RuCl$_3$(L-Pro–H)(NO)] (4). A mixture of (*n*Bu$_4$N)$_2$[RuCl$_5$NO] (350 mg, 0.44 mmol) and L-Pro (76 mg, 0.66 mmol) was refluxed in *n*-butanol (6 mL) for 3.5 h. The solvent was removed under reduced pressure. The remaining oil was dissolved in water (5 mL). The solution was transferred into a beaker and allowed to stand at room temperature. Orange crystals formed were filtered off and a second fraction was collected after 24 h. The product was washed with water/ethanol 1:1 (4 mL), diethyl ether (4 mL) and dried *in vacuo*. Yield: 94 mg, 36%. Anal. Calcd for $C_{21}H_{43}Cl_3N_3O_3Ru$ (M = 593.01 g/mol): C, 42.53; H, 7.31; N, 7.09. Found: C, 42.48; H, 7.37; N, 6.78. ESI-MS in MeOH (negative): *m/z* 352.71 [RuCl$_3$NO(L-Pro − H)]$^-$ (m_{theor} = 352.86), 314.76 [RuCl$_2$NO(L-Pro − 2H)]$^-$ (m_{theor} = 314.87), 278.69 [RuClNO(L-Pro − 3H)]$^-$ (m_{theor} = 278.91). IR, cm^{-1}: 740, 883, 1353, 1464, 1644, 1647 (vs) ν_{as}(COO$^-$), 1845 (vs) ν(NO), 2874 and 2960 (m) ν(CH), 3101 (m) ν_s(NH$_2$) and 3169 (m) ν_{as}(NH$_2$). UV−vis (buffer), λ_{max}, nm (ε, M^{-1}cm^{-1}): 279 (1981), 253 (104). ^{1}H NMR (500.32 MHz, DMSO-*d*$_6$): δ 0.95 (t, 12H_D, J = 7.4 Hz), 1.32 (sxt, 8H_C, J = 7.4 Hz), 1.58 (qui, 8H_B, J = 7.8 Hz),1.69 (m, 1H, $H_{5'}$), 1.85 (m, 2H, $H_{6'}$, $H_{5''}$), 2.05 (m, 1H, $H_{6''}$), 2.87 (m, 1H, $H_{4'}$), 3.17 (t, 8H_A J = 8.2 Hz), 3.42 (m, 1H, $H_{4''}$), 3.88 (qua, 1H, H_2, J = 7.1 Hz), 7.08 (m, 1H, H_3) ppm.

(*n*Bu$_4$N)[RuCl$_3$(D-Pro–H)(NO)] (5). A mixture of Na$_2$[RuCl$_5$NO]·6H$_2$O (400 mg, 0.86 mmol), *n*Bu$_4$NCl (450 mg, 1.62 mmol) and D-Pro (148 mg, 1.29 mmol) was refluxed in *n*-propanol (10 mL) for 2 h. The solvent was removed under reduced pressure. Water (7 mL) was added to the residue. The solution was decanted into a beaker and allowed to stand at room temperature. Orange crystals formed were filtered off after 72 h, washed with water/ethanol 1:1 (4 mL), diethyl ether (4 mL) and dried *in vacuo*. Yield: 175 mg, 34.0%. Anal. Calcd for $C_{21}H_{43}Cl_3N_3O_3Ru·0.75H_2O$ (M = 606.52 g/mol): C, 41.54; H, 7.33; N, 6.92. Found: C, 41.70; H, 7.68; N, 7.07. ESI-MS in MeOH (negative): *m/z* 351 [RuCl$_3$NO(D-Pro)]$^-$, 279 [RuClNO(D-Pro)−2HCl]$^-$. IR, cm^{-1}: 740, 883, 1353, 1464, 1644, 1647 (vs) ν_{as}(COO$^-$), 1845 (vs) ν(NO), 2874, 2960 (m) ν(CH), 3198 (m) ν(NH$_2$). UV−vis (buffer), λ_{max}, nm (ε, M^{-1}cm^{-1}): 279 (1846), 253 (90). ^{1}H NMR (500.32 MHz, DMSO-*d*$_6$): δ 0.95 (t, 12H_D, J = 7.4 Hz),

1.32 (sxt, 8H_C, J = 7.4 Hz), 1.58 (qui, 8H_B, J = 7.8 Hz),1.69 (m, 1H, $H_{5'}$), 1.85 (m, 2H, $H_{6'}$, $H_{5''}$), 2.05 (m, 1H, $H_{6''}$), 2.87 (m, 1H, $H_{4'}$), 3.17 (t, 8H_A J = 8.2 Hz),3.42 (m, 1H, $H_{4''}$), 3.88 (qua, 1H, H_2, J = 7.1 Hz), 7.08 (m, 1H, H_3) ppm.

(*n*Bu$_4$N)[RuCl$_3$(L-Ser–H)(NO)] (6). A mixture of $Na_2[RuCl_5NO]\cdot 6H_2O$ (400 mg, 0.86 mmol), *n*Bu$_4$NCl (450 mg, 1.62 mmol) and L-Ser (137 mg, 1.29 mmol) was refluxed in *n*-butanol (10 mL) for 1.5 h. The solvent was removed under reduced pressure and the remaining oil was dried *in vacuo*. The remaining oil was dissolved in water (10 mL). The solution was decanted into a beaker and allowed to stand at room temperature. Four days later orange crystals were filtered off, washed with water/ethanol 1:1 (4 mL), diethyl ether (4 mL) and dried *in vacuo*. Yield: 111 mg, 22.0%. Anal. Calcd for $C_{19}H_{42}Cl_3N_3O_4Ru$ (M = 583.98 g/mol): C, 39.08; H, 7.25; N, 7.20. Found: C, 39.30; H, 6.90; N, 6.93. ESI-MS in MeOH (negative): *m/z* 342.70 $[RuCl_3NO(L\text{-}Ser - H)]^-$ (m_{theor} = 342.84), 304.70 $[RuCl_2NO(L\text{-}Ser - 2H)]^-$ (m_{theor} = 304.87). IR, cm^{-1}: 878, 1070, 1369, 1477, 1644 (vs) $\nu_{as}(COO^-)$, 1855 (vs) ν(NO), 2875, 2956 (m) ν_a(CH), 3120 (m) $\nu_s(NH_2)$, 3190 (m) $\nu_{as}(NH_2)$ and 3448 (m) ν_s(OH). UV−vis (buffer), λ_{max}, nm (ε, $M^{-1}cm^{-1}$): 279 (1721), 453 (87). ^{1}H NMR (500.32 MHz, DMSO-*d*$_6$): δ 0.95 (t, 12H_D, J = 7.4 Hz), 1.32 (sxt, 8H_C, J = 7.4 Hz), 1.58 (qui, 8H_B, J = 7.8 Hz), 3.17 (t, 8H_A J = 8.2 Hz), 3.59 (m, 1H, $H_{4'}$), 3.75 (m, 1H, $H_{4''}$), 4.98 (m, 1H, $H_{3'}$), 5.05 (t, 1H, H_2, J = 5.35 Hz), 6.45 (m, 1H, $H_{3''}$) ppm.

(*n*Bu$_4$N)[RuCl$_3$(L-Thr–H)(NO)] (7). A mixture of $Na_2[RuCl_5NO]\cdot 6H_2O$ (400 mg, 0.86 mmol), *n*Bu$_4$NCl (450 mg, 1.62 mmol) and L-Thr (154 mg, 1.29 mmol) was refluxed in *n*-butanol (10 mL) for 1.5 h. The solvent was removed under reduced pressure and the remaining oil was dried *in vacuo*. The remaining oil was dissolved in water (10 mL). The solution was decanted into a beaker and allowed to stand at room temperature. Six days later orange crystals were filtered off, washed with water/ethanol 1:1 (4 mL), diethyl ether (4 mL) and dried *in vacuo*. Yield: 88 mg, 17.0%. Anal. Calcd for $C_{20}H_{44}Cl_3N_3O_4Ru$ (M = 598.01 g/mol): C, 40.17; H, 7.42; N, 7.03. Found: C, 40.02; H, 7.81; N, 6.78. ESI-MS in MeOH (negative): *m/z* 356.71 $[RuCl_3NO(L\text{-}Thr - H)]^-$ (m_{theor} = 356.86), 318.72 $[RuCl_2NO(L\text{-}Thr - 2H)]^-$ (m_{theor} = 318.88). IR, cm^{-1}: 592, 742, 890, 1066, 1173, 1257, 1372, 1459, 1642 (vs) $\nu_{as}(COO^-)$, 1849 (vs) ν(NO), 2875, 2966 (m) ν(CH), 3233 (m) $\nu(NH_2)$ and 3440 (m) ν(OH).

UV−vis (buffer), λ_{max}, nm (ε, $M^{-1}cm^{-1}$): 279 (1761), 453 (89). ^{1}H NMR (500.32 MHz, DMSO-d_6): δ 0.95 (t, 12H_D, J = 7.4 Hz), 1.17 (d, 3H; H_5, J = 6.75), 1.32 (sxt, 8H_C, J = 7.4 Hz), 1.58 (qui, 8H_B, J = 7.8 Hz), 3.17 (t, 8H_A, J = 8.2 Hz), 4.15 (m, 1H, H_4), 4.92 (m, 1H, $H_{3'}$), 5.16 (d, 1H, H_2, J = 5.33), 6.46 (m, 1H, $H_{3''}$) ppm.

(*n*Bu$_4$N)[RuCl$_3$(L-Tyr–H)(NO)] (8). A mixture of $Na_2[RuCl_5NO]\cdot 6H_2O$ (500 mg, 1.08 mmol), *n*Bu$_4$NCl (598 mg, 2.16 mmol) and L-Tyr (294 mg, 1.62 mmol) was refluxed in *n*-butanol (10 mL) for 2 h. The solution was allowed to cool down to room temperature, filtered and transferred into an Erlenmeyer flask. After 12 days dark-red crystals were filtered off, washed with water (5 mL), ethanol (5 mL), diethyl ether (5 mL) and dried *in vacuo*. Yield: 274 mg, 38%. Anal. Calcd for $C_{24}H_{44}Cl_3N_3O_4Ru$ (M = 660.08 g/mol): C, 45.49; H, 7.02; N, 6.37. Found: C, 45.33; H, 6.85; N, 6.12. ESI-MS in MeOH (negative): *m/z* 418.73 $[RuCl_3NO(L\text{-Tyr} - 2H)]^-$ (m_{theor} = 418.87), 380.77 $[RuCl_2NO(L\text{-Tyr} - 2H]^-$ (m_{theor} = 380.90), 344.78 $[RuClNO(L\text{-Tyr} - 3H]^-$ (m_{theor} = 344.92). IR, cm^{-1}: 740, 827, 1183, 1270, 1366, 1466, 1641 (vs) $\nu_{as}(COO^-)$, 1885 (vs) ν(NO), 2962 m ν(CH), 3101 (m) $\nu_s(NH_2)$ and 3169 (m) $\nu_{as}(NH_2)$. UV−vis (buffer), λ_{max}, nm (ε, $M^{-1}cm^{-1}$): 279 (2109), 453 (99). ^{1}H NMR (500.32 MHz, DMSO-d_6): δ 0.95 (t, 12H_D, J = 7.4 Hz), 1.32 (sxt, 8H_C, J = 7.4 Hz), 1.58 (qui, 8H_B, J = 7.8 Hz),2.96 (m, 2H, $H_{4'}$, $H_{4''}$), 3.17 (t, 8H_A J = 8.2 Hz), 3.75 (m, 1H, H_2), 4.71 (m, 1H $H_{3'}$), 6.41 (m, 1H, $H_{3''}$),6.69 (d, 2H, H_5, J = 7.4 Hz), 7.09 (d, 2H, H_5, J = 8.4 Hz), 9.22 (s, 1H, H_7) ppm.

Physical measurements. ^{1}H NMR spectra were recorded on Bruker Avance III instrument (Ultrashiled Magnet) at 500.13 MHz at room temperature. DMSO-d_6 was used as solvent. Standard pulse programs were applied. ^{1}H chemical shifts were measured relatively to the residual solvent peaks. Hydrolytic stability of complex **8** in 20 mM phosphate buffer at pH 7.4,0.1 M (KCl) ionic strength and in pure water, both containing 10% D_2O, was followed by recording ^{1}H NMR spectra over 24 h. Complex concentration was 1.0 mM. Watergate water suppression program and DSS internal standard were used. ATR-IR spectra were measured on a Bruker Vertex spectrometer. $D_{7.4}$ values were determined by the traditional shake-flask method in *n*-octanol/buffered aqueous solution at pH 7.4 (HEPES buffer) at 298.0 ± 0.2 K as described previously.[25] In the case of the complexes of L-Ala **(2)** and L -Val **(3)** the

$D_{7.4}$ values were determined in the presence of 0.1 M KCl as well. Two parallel experiments were performed for each sample. The complexes were dissolved at 0.3 mM in the *n*-octanol pre-saturated aqueous solution of the buffer (0.02 M). The aqueous solutions and *n*-octanol with 1:1 phase ratio were gently mixed with 360° vertical rotation for 3 h to avoid the emulsion formation, and the mixtures were centrifuged at 5000 rpm for 3 min by a temperature controlled centrifuge at 298 K. After separation, UV spectra of the complexes in the aqueous phase were compared to those of the original aqueous solutions, and $D_{7.4}$ values were calculated as the mean of [Absorbance (original solution) / Absorbance (aqueous phase after separation) – 1] obtained in the region of $\lambda \sim$ (250 – 290 nm).

CD and UV−vis spectra under physiological conditions (0.02 M phosphate buffer, pH 7.40 with 0.1 M KCl) were recorded on a Jasco J-815 spectrometer in an optical cell of 2 cm path length (l) in the wavelength interval from 220 to 600 nm. The analytical concentration for the CD measurement of the complexes was 50 μM in aqueous solution. CD data are given as the differences in molar absorptivities between left and right circularly polarized light, based on the concentration of the ligand ($\Delta\varepsilon = \Delta A / l / c_{complex}$). The concentrations for the UV−vis measurements amounted 403 (**1**), 401 (**4**), 401 (**5**), 400 (**8**), 399 (**3**), 401 (**2**), 403 (**7**) and 401 (**6**) μM.

ESI-MS measurements for the characterization of the complexes were carried out with a Bruker Esquire 3000 instrument; the samples were dissolved in methanol. Cyclic voltammetry measurements were performed at room temperature using an AMEL 7050 all-in one potentiostat. The concentrations amounted 1.5–2.5 mM, the samples were dissolved in acetonitrile and 0.1 to 0.2 M nBu$_4$N[BF$_4$] was added as supporting electrolyte. Further a 3 mm GC (glassy carbon electrode) working electrode, a Pt auxiliary electrode and a SCE (saturated calomel electrode) reference electrode were used. The same electrode types were used for coulometry. In this case, the compartment of auxiliary electrode was separated from the study compartment. Ferrocene was used as an internal standard.

Crystallographic Structure determination. X-ray diffraction measurements were performed on a Bruker X8 APEXII CCD diffractometer. Single crystals were

positioned at 40 mm from the detector and 1348, 1526, 1100, 2183, 961, 2191, 1606 and 1391 frames were measured, each for 30, 30, 80, 20, 10, 60, 30 and 30 s over 1 (or 0.5° for **4**) scan width for **1**–**8**, respectively. The data were processed using SAINT software.[26] Crystal data, data collection parameters, and structure refinement details are given in Tables 1 and 2. The structures were solved by direct methods and refined by full-matrix least-squares techniques. Non-hydrogen atoms were refined with anisotropic displacement parameters. H atoms were inserted in calculated positions and refined with a riding model. Two carbon atoms C5 and C6 in the tetrabutylammonium cation in **1** were found to be disordered over 3 positions with site occupation factors (s.o.f.) 0.4:0.4:0.2, while C20, C21 and C22 in one of six crystallographically independent TBA cations in **2** over two positions with s.o.f. 0.5:0.5. In complex **4** the C2 atom of the prolinic ring and atoms C6 and C8 of L-Ser in one crystallographically independent complex anion in **6** were found to be disordered over two positions with populations 0.8:0.2. The carbon atoms C12, C13, C16, C17, C21 and C24, C25 in the TBA cation in **8** were found to be disordered over 2 positions with s.o.f. 0.6:0.4. The disorder was resolved by using restraints SADI and EADP implemented in SHELXL. The following computer programs and hardware were used: structure solution, *SHELXS-97* and refinement, *SHELXL-97*[27]; molecular diagrams, ORTEP[28]; computer, Intel CoreDuo.

Mass Spectrometry. The stability of four compounds, namely **1**, **4**, **5** and **8** in aqueous solution and in the presence of 4 equiv sodium ascorbate was investigated using an AmaZon SL ESI ion trap mass spectrometer (Bruker Daltonics GmbH, Bremen, Germany). For this purpose, the compounds were diluted from 400 μM stock solution (1% DMSO) to 50 μM in water and in the presence of 200 μM sodium ascorbate. The solutions were incubated at 37 °C in the dark and samples were measured after 0.5, 1, 2, 6 and 24 h after a second dilution step to 5 μM of the metal compound. The samples were introduced by direct infusion into the mass spectrometer at 280 μL/h and mass spectra were recorded over 0.5 min and averaged. Typical experimental conditions were as follows: HV capillary ±4.5 kV, dry temp 180 °C, nebulizer 8 psi, dry gas 6 L/min, RF level 77%, trap drive 57.6, average accumulation time 25 ms (negative ion mode) and 120 μs (positive ion mode). Mass spectra were acquired and processed using ESI Compass 1.3 and DataAnalysis 4.0

(Bruker Daltonics GmbH, Bremen, Germany). The theoretically most abundant signal of isotopic pattern is annotated.

Antiproliferative activity. CH1 cells (human ovarian carcinoma) were a generous gift from Lloyd R. Kelland, CRC Centre for Cancer Therapeutics, Institute of Cancer Research, Sutton, UK. SW480 (human adenocarcinoma of the colon) and A549 (human nonsmall cell lung cancer) cells were kindly provided by Brigitte Marian (Institute of Cancer Research, Department of Medicine I, Medical University of Vienna, Austria). All cell culture media and reagents were purchased from Sigma-Aldrich Austria and plastic ware from Starlab Germany. Cells were grown in 75 cm^2 culture flasks as adherent monolayer cultures in Minimum Essential Medium (MEM) supplemented with 10% heat-inactivated fetal calf serum, 1 mM sodium pyruvate, 4 mM L-glutamine and 1% non-essential amino acids (from 100x ready-to-use stock). Cultures were maintained at 37 °C in humidified atmosphere containing 95% air and 5% CO_2.

Cytotoxic effects of the test compounds were determined by means of a colorimetric microculture assay [MTT assay; MTT = 3-(4,5-dimethyl-2-thiazolyl)-2,5-diphenyl-2H-tetrazolium bromide] as described previously.[13] Cells were harvested from culture flasks by trypsinization and seeded by using a pipetting system (Biotek Precision XS Microplate Sample Processor) in densities of 1×10^3 (CH1), 2×10^3 (SW480) and 3×10^3 (A549) in 100 μL/well aliquots in 96-well microculture plates. For 24 h, cells were allowed to settle and resume proliferation. Test compounds were then dissolved in DMSO, diluted in complete culture medium and added to the plates where the final DMSO content did not exceed 0.5%. After 96 h of drug exposure, the medium was replaced with 100 μL/well of a 1:7 MTT/RPMI 1640 mixture (MTT solution, 5 mg/mL of MTT reagent in phosphate-buffered saline; RPMI 1640 medium, supplemented with 10% heat-inactivated fetal bovine serum and 4 mM L-glutamine), and plates were incubated for further 4 h at 37 °C. Subsequently, the solution was removed from all wells, and the formazan crystals formed by viable cells were dissolved in 150 μL of DMSO per well. Optical densities at 550 nm were measured with a microplate reader (Biotek ELx808) by using a reference wavelength of 690 nm to correct for unspecific absorption. The quantity of viable cells was expressed relative to untreated controls, and 50% inhibitory concentrations (IC_{50}) were

calculated from concentration-effect curves by interpolation. Evaluation is based on means from three independent experiments.

Results and Discussion

We were interested in the study of the reactions of ruthenium-nitrosyl complexes with all amino acids except two already reported in the literature with L-His and L-Met,[10,11] isolation of the resulted products and testing antiproliferative activity of all prepared products, including $[RuCl_2(L\text{-His}–H)(NO)]$ and $[RuCl_2(L\text{-Met}–H)(NO)]$, reported previosly. Amino acids are potential biological ligands for ruthenium anticancer drugs. The interactions with amino acids deserve to be investigated, as they can help in elucidating the underlying mechanism of their antitumor activity. These reactions and the biological effects of the resulting species are still little understood.

It is known, however, that cisplatin and carboplatin have a high affinity for sulfur-containing biological molecules, such as methionine, glutathione and sulfur containing proteins. These interactions have been associated with toxic side effects, detoxification and resistance mechanisms, as well as with delivery of active species to the cell for ultimate binding to DNA.[23a,29,30,31]

In the case of ruthenium, it has been found that $[(\eta^6\text{-bip})Ru(en)Cl][PF_6]$ (bip = biphenyl, en = ethylenediamine) reacts slowly with L-Cys, L-Met and L-His in water at 310 K to partial (22–50%) completion.[32,33] Comparison of the equilibrium constants measured suggested that the affinity of the $[(\eta^6\text{-bip})Ru(en)]^{2+}$ moiety for these amino acids decreases in the order L-Cys > L-Met > L-His.[34] The observed reactions were largely suppressed in the presence of 0.1 M NaCl indicating that these amino acids may not be able to inactivate the complex in blood plasma or in cells.[30] The low reactivity of these amino acids towards $[(\eta^6\text{-bip})Ru(en)Cl][PF_6]$ may be the reason for low toxic side effects of this and related ruthenium-arene complexes.[35] These interactions cannot impede the transport and delivery of the drugs to the cancer cells and allow at least for some amino acids to act as drug reservoirs for DNA ruthenation.[33] In stark contrast, ruthenium hexacationic prism reacts with His, which binds to Ru(η^6-*p*-cymeme) moiety with release of the 2,4,6-tri(pyridin-4-yl)-1,3,5-triazine and 1,4-benzoquinonato ligands, while it remains intact in the presence of Met.[36] The resulting (*p*-cymene)Ru-His complex was found to catalyze oxidation of

cysteine to cystine more efficiently than the original complex, and this process may play a role in the aniproliferative activity of the complex since amino acids represent a significant part of cytosol. Sequence-specific catalytic peptide synthesis with the half-sandwich ruthenium complex is another example well-documented in the literature.[37] NAMI-A treated with histidine or glutamine at their minimum essential medium (MEM) concentrations was shown to result in a reduced uptake by KB carcinoma cells presumably because of formation of adducts with these amino acids or competition between MEM components and NAMI-A upon transport through the cell membrane.[38] So reactions with amino acids may also have an impact on intracellular chemistry of ruthenium-based drugs.

In this work we report on the preparation of 8 ruthenium-nitrosyl complexes with Gly, L-Ala, L-Val, L-Pro, D-Pro, L-Ser, L-Thr and L-Tyr. As starting material $Na_2[RuCl_5(NO)]\cdot 6H_2O$ was used, which was prepared by reaction of $RuCl_3\cdot nH_2O$ with $NaNO_2$ in the presence of 6 M HCl as reported previously, or $(n\text{Bu}_4\text{N})_2[RuCl_5(NO)]$.[24] Complexes **1**−**8** were synthesized by boiling $Na_2[RuCl_5(NO)]\cdot 6H_2O$ with 1.5 equiv tetrabutylammonium chloride and 1.1 equiv of the corresponding amino acid or by reaction of $(n\text{Bu}_4\text{N})_2[RuCl_5(NO)]$ with AA in *n*-butanol or *n*-propanol with 15 to 38% yields. Compounds **1** and **8** crystallized directly from the reaction mixture after its completion. All other complexes were obtained by evaporating the solvent under reduced pressure and re-crystallization of the residue from water at room temperature over 96 h on average. ESI mass spectra measured in positive ion mode showed a peak at *m*/*z* 242 due to $n\text{Bu}_4\text{N}^+$, while those measured in negative ion mode showed strong peaks at *m*/*z* 312, 324, 353, 351, 351, 342, 355 and 419 for **1**−**8**, respectively, attributed to $[Ru(NO)Cl_3(AA-H)]^-$. Other signals of moderate intensity usually found in the mass spectra were assigned to $[RuCl_2(AA-H)(NO)-2H]^-$ and $[RuCl(AA-H)(NO)-3H]^-$. Coordination of an amino acid to ruthenium in $[RuCl_5(NO)]^{2-}$ leads to a shift of stretching vibration ν(NO) from 1902 cm^{-1} to 1837−1852 cm^{-1} for **1**−**8**. All complexes are diamagnetic. The number of proton resonances in ^1H NMR spectra of **1**−**8** in DMSO-d^6 is in accordance with the proposed structures for these compounds (see Chart 1 and experimental section).

X-ray Crystallography. As reported for osmium-nitrosyl complexes with Gly, L-Pro and D-Pro,[13] three isomeric structures are theoretically possible for

$[RuCl_3(AA{-}H)(NO)]^-$ (AA = Gly, L-Ala, L-Val, L-Pro, D-Pro, L-Ser, L-Thr and L-Tyr acting as bidentate ligands): one *fac*-isomer with three chlorido ligands coordinated to ruthenium in facial configuration and two others with three chlorido ligands bound to central atom in meridional fashion. In the first hypothetical meridional isomer NO is located in *trans* position to the N atom of the amino acid, while in the second NO is bound in *trans* position to the carboxylic oxygen atom of the AA ligand. According to X-ray crystallography all studied compounds (**1**–**8**) have a similar ionic crystal structure, which is built up from coordination anions $[RuCl_3(AA{-}H)(NO)]^-$ and tetrabutylammonium cations. No co-crystallized solvent has been found in the crystals of compounds studied, except the structures **2** and **6**, which contain some statistically distributed water molecules. The results of X-ray diffraction studies of complexes **1**–**8** together with atom numbering schemes are shown in Figures 1–3. The crystallographic data and refinement details are given in Tables 1 and 2, while selected geometrical parameters in Table 3. The asymmetric part in **6** and **7** contains two, while in **2** six chemically identical but crystallographically independent cation/anion pairs. Figures 1b, 3a and 3b show the structures of only one asymmetric component in the unit cell.

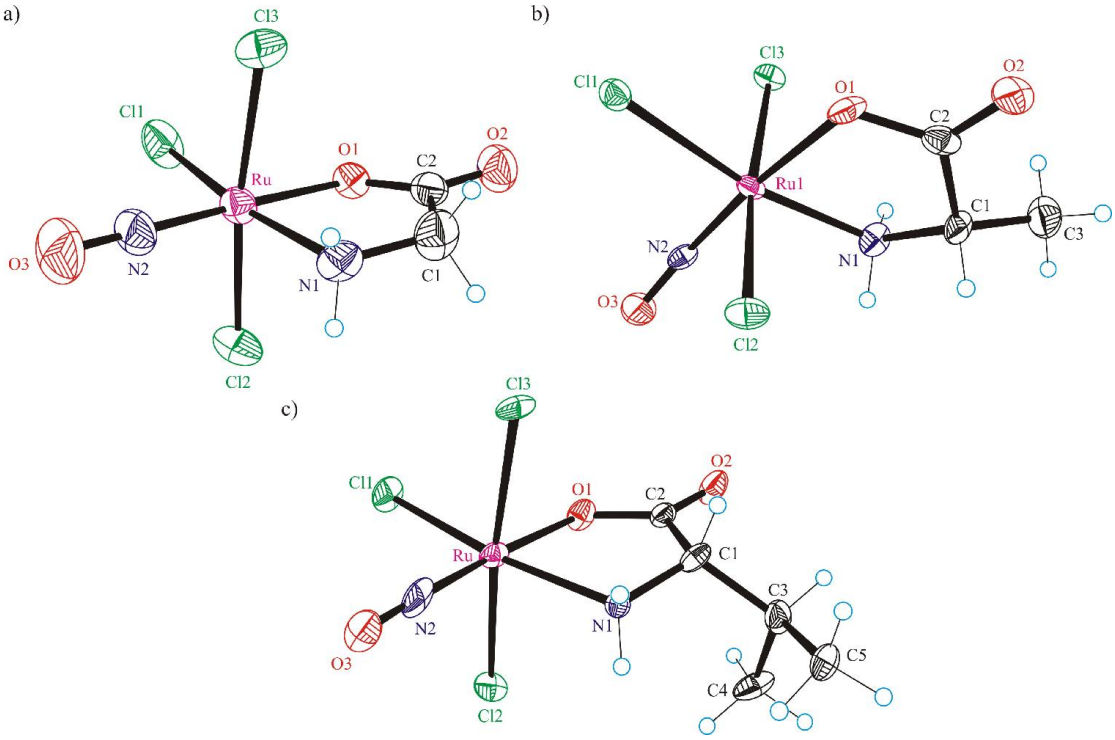

Figure 1. ORTEP drawings of the complex anion $[RuCl_3(Gly{-}H)(NO)]^-$ in **1** (a), $[RuCl_3(L\text{-}Ala{-}H)(NO)]^-$ in **2** (b), and $[RuCl_3(L\text{-}Val{-}H)(NO)]^-$ in **3** (c) with atom labeling. The thermal ellipsoids are drawn at 50% probability level.

Table 1. Crystal Data and Details of Data Collection for complexes **1**−**4**.

Complex	**1**	**2**	**3**	**4**
empirical formula	$C_{18}H_{40}Cl_3N_3O_3Ru$	$C_{19}H_{42.34}Cl_3N_3O_{3.17}Ru$	$C_{21}H_{46}Cl_3N_3O_3Ru$	$C_{21}H_{44}Cl_3N_3O_3Ru$
Fw	553.95	570.98	596.03	594.01
space group	$Pna2_1$	$P2_1$	$P2_12_12_1$	$P2_12_12_1$
a, [Å]	10.1942(5)	15.3062(8)	8.6937(8)	10.2263(4)
b, [Å]	16.8268(9)	17.0885(8)	13.8069(12)	15.6517(6)
c, [Å]	15.6678(8)	31.3660(16)	22.711(2)	17.9281(7)
β, [°]		91.371(3)		
V [Å^3]	2687.6(2)	8201.7(7)	2726.1(4)	2869.55(19)
Z	4	12	4	4
λ [Å]	0.71073	0.71073	0.71073	0.71073
ρ_{calcd}, [g cm^{-3}]	1.369	1.387	1.452	1.375
crystal size, [mm^3]	0.08 × 0.07 × 0.05	0.20 × 0.15 × 0.05	0.15 × 0.05 × 0.05	0.20 × 0.18 × 0.10
T [K]	293(2)	100(2)	100(2)	120(2)
μ, [mm^{-1}]	0.902	0.890	0.895	0.850
R_1[a]	0.0321	0.0566	0.0634	0.0147
wR_2[b]	0.0844	0.1346	0.1656	0.0418
Flack parameter	−0.02(5)	0.02(3)	0.01(8)	0.015(16)
GOF[c]	1.001	1.132	1.092	1.025

[a] $R_1 = \Sigma||F_o| - |F_c||/\Sigma|F_o|$. [b] $wR_2 = \{\Sigma[w(F_o^2 - F_c^2)^2]/\Sigma[w(F_o^2)^2]\}^{1/2}$. [c] GOF = $\{\Sigma[w(F_o^2 - F_c^2)^2]/(n - p)\}^{1/2}$, where n is the number of reflections and p is the total number of parameters refined.

Table 2. Crystal Data and Details of Data Collection for Complexes **5**–**8**.

Complex	**5**	**6**	**7**	**8**
empirical formula	$C_{21}H_{44}Cl_3N_3O_3Ru$	$C_{19}H_{42.15}Cl_3N_3O_{4.08}Ru$	$C_{20}H_{44}Cl_3N_3O_4Ru$	$C_{25}H_{46}Cl_3N_3O_4Ru$
Fw	594.01	585.33	598.00	660.07
space group	$P2_12_12_1$	$P1$	$P2_1$	$P2_12_12_1$
A, [Å]	10.1919(19)	9.7963(4)	12.6677(12)	9.9542(3)
B, [Å]	15.628(3)	10.7133(4)	10.7195(10)	17.1180(6)
C, [Å]	17.930(4)	13.6446(6)	20.253(2)	17.8215(6)
α, [°]		75.440(2)		
β, [°]	2855.9(10)	85.146(2)	102.943(5)	
γ, [°]	4	79.953(2)		
V [Å^3]	0.71073	1363.52(10)	2680.3(4)	3036.71(17)
Z	1.382	2	4	4
λ [Å]	0.30 × 0.05 × 0.03	0.71073	0.71073	0.71073
ρ_{calcd}, [g cm^{-3}]	120(2)	1.426	1.482	1.444
crystal size, [mm^3]	0.854	0.15 × 0.10 × 0.08	0.30 × 0.10 × 0.06	0.20 × 0.10 × 0.07
T [K]	0.0539	100(2)	100(2)	120(2)
μ, [mm^{-1}]	0.1326	0.896	0.913	0.814
R_1[a]	0.05(6)	0.0211	0.0430	0.0318
wR_2[b]	1.010	0.0508	0.1110	0.0816
Flack parameter		0.01(1)	–0.06(2)	0.01(3)
GOF[c]		1.003	1.065	1.003

[a] $R_1 = \Sigma||F_o| - |F_c||/\Sigma|F_o|$. [b] $wR_2 = \{\Sigma[w(F_o^2 - F_c^2)^2]/\Sigma[w(F_o^2)^2]\}^{1/2}$. [c] GOF = $\{\Sigma[w(F_o^2 - F_c^2)^2]/(n - p)\}^{1/2}$, where n is the number of reflections and p is the total number of parameters refined.

Table 3. Selected bond distances (Å) and bond angles in **1**–**8**.

Atom1–Atom2	**1**	**2**[a]	**3**	**4**	**5**	**6**[b]	**7**[b]	**8**
Ru–O1	2.001(3)	2.009(5), 1.993(9)	1.997(5)	1.998(1)	1.988(4)	2.008(2), 2.011(3)	2.011(3), 2.009(1)	2.019(3)
Ru–N1	2.051(4)	2.078(6), 2.073(4)	2.097(6)	2.107(2)	2.132(6)	2.068(1), 2.074(7)	2.078(3), 2.086(8)	2.077(3)
Ru–N2	1.702(4)	1.707(6), 1.714(3)	1.731(7)	1.725(2)	1.726(6)	1.7256(17), 1.7249(7)	1.732(4), 1.729(3)	1.730(3)
N2–O3	1.149(6)	1.178(8), 1.164(7)	1.158(8)	1.147(2)	1.141(7)	1.149(2), 1.1485(5)	1.145(5), 1.147(2)	1.137(3)
Ru–Cl1	2.361(2)	2.376(2), 2.367(3)	2.363(2)	2.3756(4)	2.383(2)	2.3724(4), 2.374(1)	2.365(1), 2.369(4)	2.3771(7)
Ru–Cl2	2.361(2)	2.370(2), 2.381(6)	2.376(2)	2.3803(4)	2.368(2)	2.3539(4), 2.36(1)	2.367(1), 2.3664(9)	2.3713(8)
Ru–Cl3	2.380(1)	2.364(2), 2.360(5)	2.374(2)	2.3636(5)	2.383(2)	2.3789(4), 2.37(3)	2.376(1), 2.371(4)	2.3732(6)
Atom1–Atom2–Atom3								
O1–Ru–N1	80.1(1)	80.0(2), 81.0(4)	80.5(2)	80.67(5)	81.4(2)	79.35(6), 79.2(1)	80.0(1), 79.7(3)	81.28(9)
Ru–N2–O3	179.1(5)	171.9(6), 176(1)	177.7(6)	176.52(16)	176.4(6)	178.30(15), 177.5(9)	174.1(3), 174.8(7)	179.4(3)
Cl2–Ru–Cl3	172.77(5)	173.71(7), 173.1(5)	173.96(8)	174.90(2)	175.37(7)	172.42(2), 172.9(5)	173.93(4), 173.1(6)	172.74(3)

[a]Parameters for one of the six crystallographically independent complex anions and average values are quoted. [b]Parameters for one of the two crystallographically independent complex anions and average values are quoted.

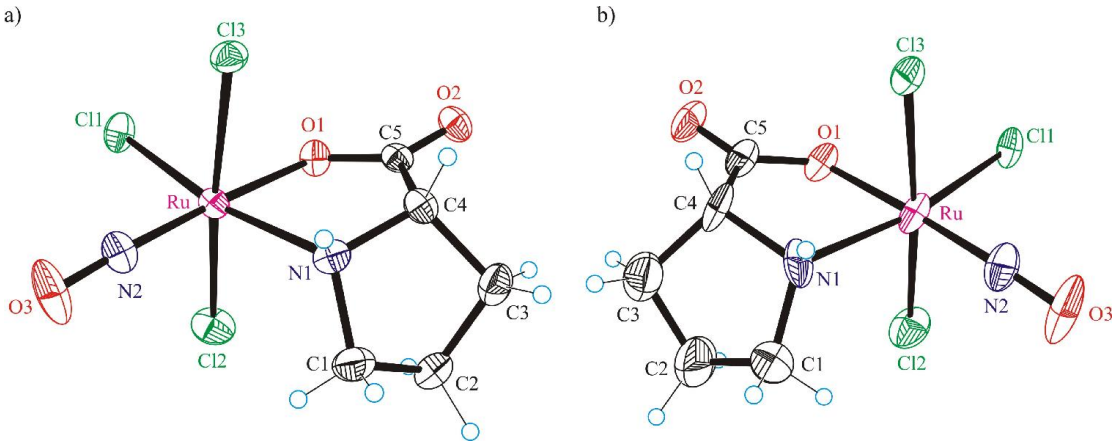

Figure 2. ORTEP drawings of the complex anion $[RuCl_3(L\text{-}Pro–H)(NO)]^-$ in **4** (a), and $[RuCl_3(D\text{-}Pro–H)(NO)]^-$ in **5** (b) with atom labeling. The thermal ellipsoids are shown at 50% probability level.

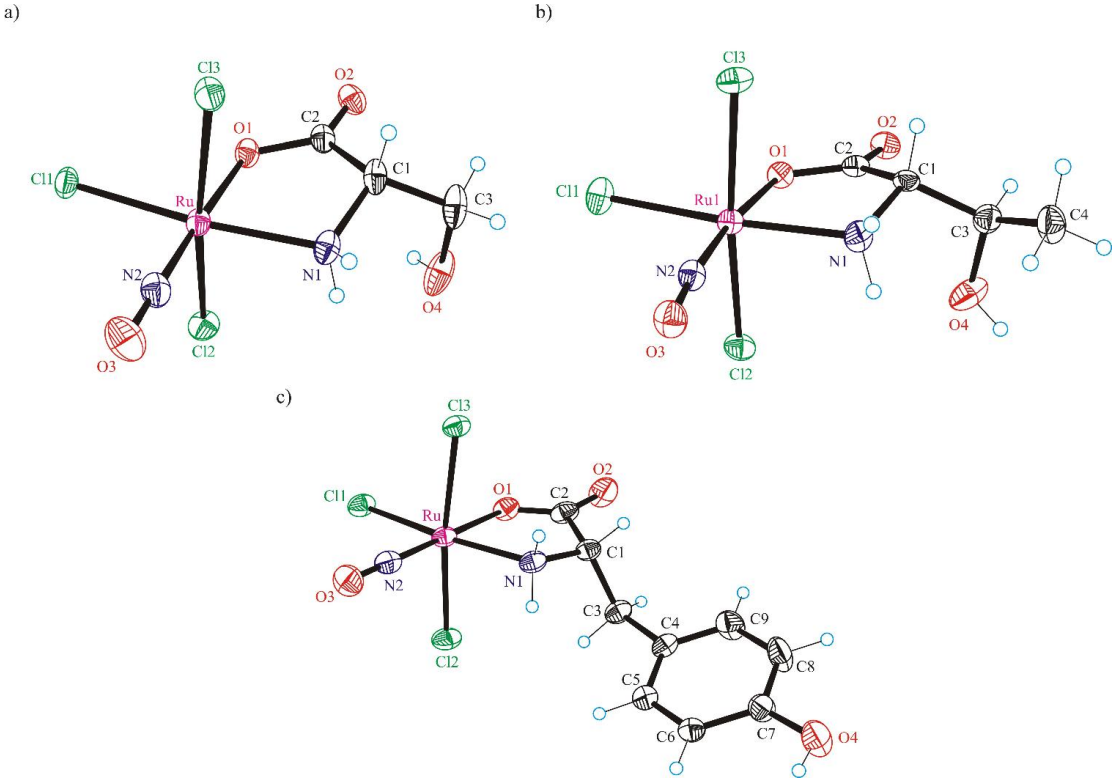

Figure 3. ORTEP drawings of the complex anion $[RuCl_3(L\text{-}Ser–H)(NO)]^-$ in **6** (a), $[RuCl_3(L\text{-}Thr–H)(NO)]^-$ in **7** (b), and $[RuCl_3(L\text{-}Tyr–H)(NO)]^-$ in **8** (c) with atom labeling. The thermal ellipsoids are shown at 50% probability level.

Each ruthenium atom in **1–8** adopts a slightly distorted octahedral coordination geometry, being coordinated by $(AA–H)^-$ nitrogen atom and carboxylate oxygen donor, one nitrosyl and one chlorido ligands in the equatorial plane and two Cl^-

ligands in axial positions. Three chlorido ligands are bound meridionally with the average distances Ru–Cl at 2.37 Å. The NO ligand is coordinated almost linearly to ruthenium on *trans* position to the carboxylic oxygen atom of the $(AA–H)^-$ ligand with the Ru–O bond length of about 1.71 Å (see Table 3). The equatorial coordination plane is practically planar. The maximum deviation from the mean-square plane in all structures does not exceed ±0.03 Å. In the structures **1** and **8** the five-membered chelate ring formed upon the coordination of $(AA–H)^-$ is almost planar, while in all other cases it adopts a half-chair conformation. Thus, in **2**, **3**, **6** and **7** the angle between Ru1O1C2C1 and Ru1N1C1 planes is equal to 24.8° 18.9°, 29.8° 24.6°, while between Ru1O1C4C5 and Ru1N1O1 in **4** and **5** to 17.1°, 17.5°, respectively. As found in earlier reported osmium complexes,[13] the two chiral centers located on C1 and N1 atoms have the same configuration S_CS_N and R_CR_N in **4** and **5**, respectively. The configuration of asymmetric atoms C1 and C3 of L-Thr is also preserved in the complex **7**. Selected bond lengths and angles summarized in Table 3 suggest that there are no marked geometrical parameter variations among the complexes **1**–**8**.

There are different groups which can play the role of potential proton donors or proton acceptors in the crystal structures **1**–**8**. The relevant hydrogen bonding parameters are collected in Table S1. The common crystal structure motif for **1**–**8** is determined by the parallel packing of one-dimensional polymeric chains, assembled via hydrogen bonding of the complex anions. The perspective views of these supramolecular architectures are shown in Figures S1–S4. These chains are of four types depending on the nature of hydrogen bonding interactions. Figure S1 shows infinite chains formed in crystals of **1**–**3** via N–H···Cl contacts. Polymeric chains in complexes **4**–**6** are built up via H-bonds of two types N–H···O and N–H···Cl as shown in Figure S2, while those in complexes **7** and **8** shown in Figures S3 and S4 are formed via interactions of the types N–H···O, O–H···O and N–H···Cl, O–H···O, respectively. Note, that all possibilities for hydrogen bonding formation are exhausted in **1**–**8**.

The diamagnetic behavior of **1**–**8**, the ν_{NO} wavenumbers and the linearity of Ru–NO group provide strong evidence for the formulation $\{Ru(NO)\}^6$ containing Ru^{II} ($S = 0$) bound to NO^+ ($S = 0$) or Ru^{III} ($S = ½$) coupled antiferromagnetically to NO^0 ($S = ½$).

Electrochemistry. The redox properties of complexes **2**–**8** have been investigated by cyclic voltammetry at a glass carbon electrode in a 0.1–0.2 M [nBu$_4$N][BF$_4$]/CH$_3$CN solution at 25 °C. For **3–7** similar electrochemical behavior was observed as shown in Figures S5−S8. The compounds show one to three irreversible oxidation waves with peak potential values higher than 1.6 V *vs.* SCE (Table 4). At these potentials, the ruthenium(II) ion is usually oxidized.[39] The processes are irreversible due to chemical reactions that follow the electron transfer(s). The oxidation of the metal-bound amino acid is largely depending on the experimental conditions.[40] Dissociation of the amino acid from ruthenium results in the formation of electrode deposit. This was encountered upon several coulometry experiments performed. The number of electrons involved in all the oxidation waves (determined by coulometry or with the use of the Fc^+/Fc couple as reference) gave generally an apparent electron number n_{app} = 3. A similar value was found for [Os(NO)Cl$_3$(AA)]$^-$ (AA = amino acid), with one irreversible electron transfer followed by one reversible process.[13] For osmium complexes, the peak separation was dependent on the nature of the coordinated amino acid. In addition, the reaction [Os(NO)]^6 → [Os(NO]^5, generally reversible or quasi-reversible, could also be identified. Here, all the processes are irreversible and the accurate determination of the peak potential values depends on the degree of the overlapping of the oxidation waves. In particular, for **3** (Figure S5) a more distinct separation of the oxidation waves (at *ca.* 1.90 and 2.30 V *vs.* SCE) is observed than for **6** (1.80 and 1.87 V *vs.* SCE). Taking all this into account we suggest that the anodic waves can be attributed to both the oxidation of ruthenium ion and the oxidation of the amino acid. Upon reduction we observe a one-electron irreversible wave at ca. –0.8 V *vs.* SCE (except for **3** and **8**). Note that more positive values were seen for related osmium complexes.[13] This reduction process presumably takes place on the metal center and is followed by chemical transformations. For **3** the general pattern of reduction peaks seems to be dependent on the state of the electrode area (see Figure S5).

Table 4. Cyclic voltammetric data[a] for complexes **2**–**8.**

Compound	Oxidation peaks			Reduction peaks[b]
2	[d]			−0.79
3	1.8[sh]	1.90	2.28	−1.31
4	1.63[c]			−0.79
5	1.68[c]			−0.82
6	1.8[sh]	1.87		−0.80
7	1.8[sh]	1.91		−0.83
8	[d]			−2.25

[a] Potential values in Volt ± 0.02 vs SCE, in a 0.1–0.2 M [nBu$_4$N][BF$_4$]/CH$_3$CN solution, at a GC working electrode, determined by using the [Fe(η^5-C$_5$H$_5$)$_2$]$^{0/+}$ redox couple ($E_{1/2}^{ox}$ = 0.525 V vs SCE)[41,42] as internal standard at a scan rate of 100 mVs^{-1}; the values can be converted to the NHE reference by adding +0.245 V. [b]determined in the experiment with several cycles of potential; [c]in comparison with the ferrocene these values are close. [d] no clear oxidation wave was observed; sh = shoulder.

UV–vis and CD spectra. The complexes possess fairly similar UV−vis spectra with a well-defined λ_{max} at 452 nm (Figure 4).

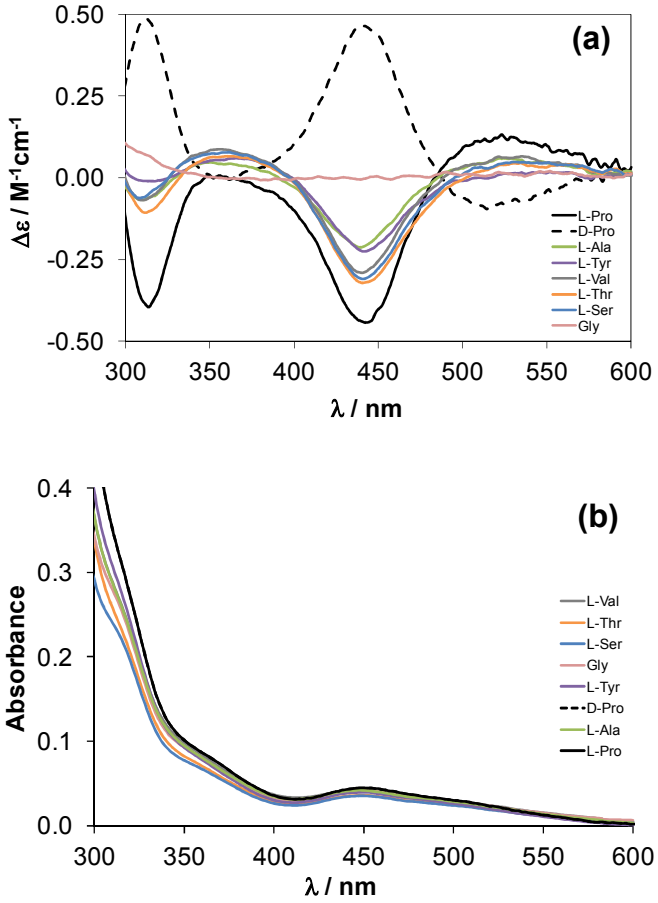

Figure 4. CD (a) and UV−vis (b) spectra of the studied (nBu$_4$N)[RuCl$_3$(AA–H)(NO)] complexes at pH 7.40 [$c_{complex}$ = 50 μM; 0.02 M phosphate buffer; 0.1 M KCl; T = 298 K].

CD spectra of the complexes of the L-amino acids show similarities as well, namely negative peaks with λ_{max} at ~ 440 and 313 nm, while the complex of D-Pro shows positive peaks at the same wavelengths.

Hydrolytic stability, lipophilicity and co-incubation with sodium ascorbate. The hydrolytic stability of complex **8** was monitored in aqueous medium buffered at pH 7.4, 0.1 M KCl by ^{1}H NMR spectroscopy over 24 h. Chemical shifts and shape of all peaks remained unchanged within this time frame (see Figure S9). In addition a solution of complex **8** in 10% D_2O/H_2O mixture in non-buffered medium (pH = 5.86) showed the same NMR spectra as solutions buffered at pH 7.4. Hydrolytic stability of complexes **1–8** were further investigated by UV−vis spectroscopy (*vide infra*).

All the prepared complexes were found to be moderately water soluble and stable in solution within the time frame of the measurements (5.5 h), since the normalized UV−vis spectra recorded after the partitioning were identical with the original ones. It is noteworthy that hydrolysis of complexes **5** and **8** is negligible over 24 h in the presence of 0.1 M KCl or in its absence as illustrated in Figure 5.

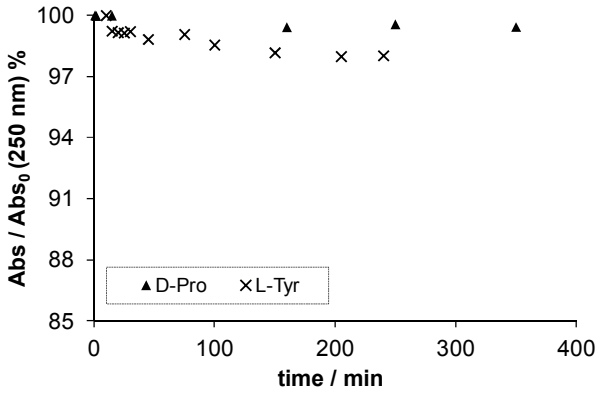

Figure 5. Time dependence of absorbance values of $(Bu_4N)[RuCl_3(AA–H)(NO)]$ complexes, where AA = D-Pro and L-Tyr recorded at 250 nm at pH 7.40 [$c_{complex}$ = 0.25 mM; 0.02 M HEPES; T = 298.0 K].

The log$D_{7.4}$ values of the complexes were determined by the traditional shake-flask method in *n*-octanol/buffered aqueous solution at pH 7.4 by analysis of the UV−vis spectra of the aqueous phases before and after separation (Figure S10, Table 5). Results revealed the fairly hydrophilic character of all the complexes studied. The log$D_{7.4}$ values for the complexes increase in the following order: Gly (**1**) < L-Ser (**6**),

L-Thr (**7**), L-Ala (**2**) < D/L-Pro (**5/4**) < L-Tyr (**8**), L-Val (**3**) corresponding well to the expectations based on the hydrophilicity of the side chains of the coordinated amino acids. On the other hand the presence of chloride ion does not alter significantly the lipophilicity of the complexes (Table 5).

The aqueous stability of compounds **1**, **4**, **5** and **8** was also confirmed by ESI mass spectrometry. Mass spectra recorded in the negative ion mode revealed $[RuCl_3(AA - H)NO]^-$ as the major species (Figures S11–S13) in all four incubations over 24 h, while TBA was the only mass signal in the positive ion mode. Similar mass spectra were observed for the co-incubation with 4 equiv sodium ascorbate, a potent biological reducing agent. These results largely parallel the findings with analogous osmium-nitrosyl complexes with amino acids, which were also stable in water.[13] In the present study, however, an additional mass signal was assigned to $[RuCl(AA - H)NO - 2H]^-$ and probably stems from the spraying process. The simultaneous cleavage of two HCl molecules from the parent mass signal during ionization indicates that the ruthenium compounds might be activated by hydrolysis. This would also be in line with the increased antiproliferative activity of the $[RuCl(AA - H)NO]^-$ series compared to the osmium counterparts. Obviously, compound **1** does only have 4 hydrogen atoms stemming from the coordinated Gly–H. We performed ESI-MS experiments of **1** in D_2O and H_2O, respectively, in order to investigate, which hydrogens are abstracted to provide the negative charge of this gas-phase compound (Figure 6). Dissolution of **1** in D_2O leads to the exchange of the labile $–NH_2$ to $–ND_2$ and the resulting compound $[RuCl_3(N,N\text{-}d_2\text{-Gly} - H)NO]^-$ (*m/z* 314.74 compared to *m/z* 312.72 of **1**) was analyzed. As can be seen in Figure 6 in a first step DCl is cleaved from the parent ion following the deprotonation of the coordinated amine. The cleavage of HCl in the second step suggests imine formation.

Incubation with sodium ascorbate did not induce ligand release over 24 h. Note that related ruthenium-nitrosyl complexes with azole heterocycles reacted quantitatively with sodium ascorbate within several hours.[15]

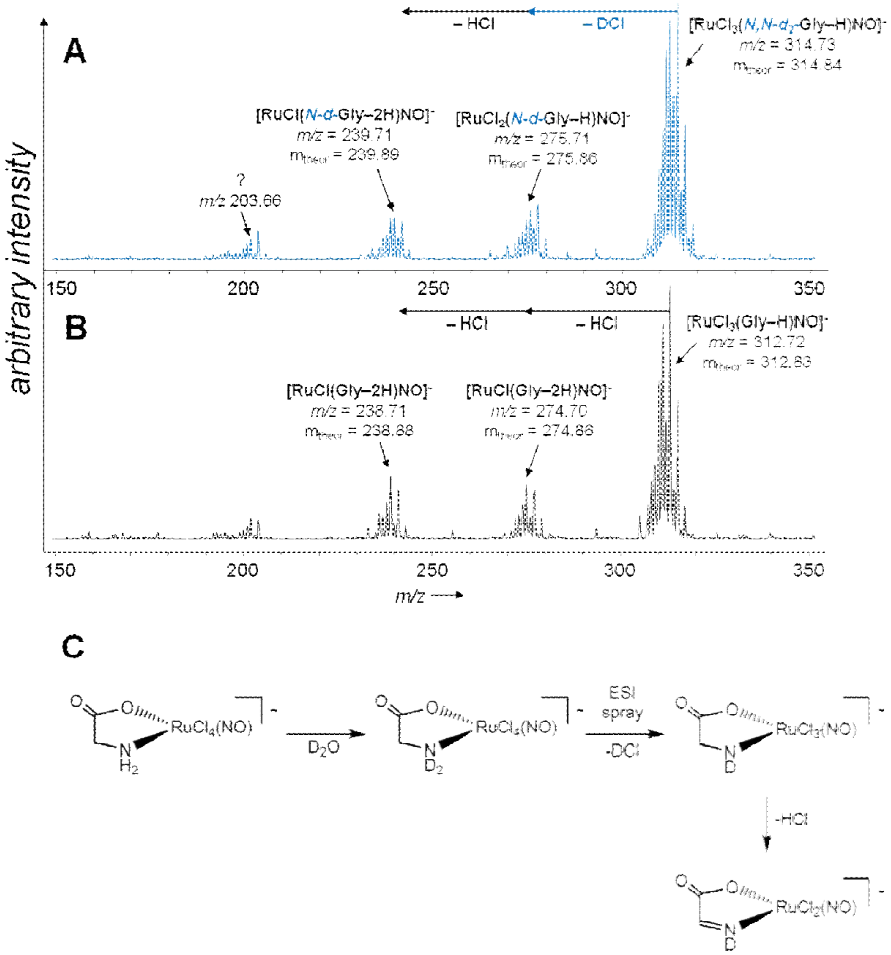

Figure 6. ESI mass spectra of **1** in D_2O (A) and H_2O (B) are shown. Dissolution of **1** in D_2O leads to the exchange of the labile hydrogen atoms of the amino group by deuterium introducing two neutrons in the compound increasing the molecular mass. The mass-to-charge ratio of the fragments indicates the position of H/D abstraction (C).

Inhibition of cancer cell growth. The *in vitro* anticancer activity of complexes **1**–**8** was assessed in human cancer cell lines CH1 (ovarian carcinoma), SW480 (colon carcinoma) and A549 (nonsmall cell lung carcinoma) by means of the colorimetric MTT assay, yielding the IC_{50} values listed in Table 5. All compounds show a higher effect in the generally more chemosensitive CH1 cells (IC_{50}: 7.5–27 µM) than in SW480 cells (IC_{50}: 20–71 µM) and the generally more chemoresistant A549 cells (IC_{50}: > 100 µM). With regard to variation of the amino acid ligand, differences between IC_{50} values within each of the cell lines CH1 and SW480 are all smaller than fourfold. In CH1 cells, the IC_{50} is 3.6 times higher for the glycinato complex **1,** which

is the most hydrophilic compound, than for the L-valinato complex **3**, which is the most hydrophobic compound. The L-prolinato (**4**) and D-prolinato (**5**) analogs show differences in antiproliferative activity, with the latter being more active than the former by factors of 1.5 and 2.7 in CH1 and SW480 cells, respectively. Overall, complex **5** shows the strongest growth inhibitory effect in all three cancer cell lines.

The antiproliferative activity of these ruthenium complexes is particularly remarkable in comparison with osmium analogs published previously.[13] The ruthenium complex (nBu$_4$N)[RuCl$_3$(Gly–H)(NO)] (**1**) turned out to be more active than corresponding osmium analog (n-Bu$_4$N)[Os(NO)Cl$_3$(Gly)] with a maximum factor of 12 in CH1 cells (3.6 and 3.2 in SW480 and A549 cells, respectively). In the mentioned publication the (n-Bu$_4$N)[Os(NO)Cl$_3$(L-Pro)] and (n-Bu$_4$N)[Os(NO)Cl$_3$(D-Pro)] complexes did not show pronounced activity and no differences between isomers. In contrast, the complexes (nBu$_4$N)[RuCl$_3$(L-Pro–H)(NO)] and (nBu$_4$N)[RuCl$_3$(D-Pro–H)(NO)] presented here show pronounced effects and a slight dependence on L-/D-isomerism. The D-isomer is 11-fold and 14-fold more active in CH1 and SW480 cells, respectively, whereas the L-isomer is 5.7-fold and 4.4-fold more active than the respective osmium analog. A synopsis of all comparisons reveals that the impact of changing the metal center on cytotoxic potency is much bigger than that of varying the amino acid ligand.

Table 5. *In vitro* anticancer activity of the compounds **1**−**8** and three osmium analogues **1*, 4*** and **5*** in human ovarian (CH1), colon (SW480) and non-small cell lung (A549) carcinoma cell lines and log$D_{7.4}$ values for the complexes; 50% inhibitory concentrations (means ± standard deviations), obtained by the MTT assay (exposure time 96 h), log$D_{7.4}$ values were estimated in 0.02 M HEPES; T = 298.0 K.

IC_{50} values ± SD (μM)				Partition coefficients	
Complex	A549	CH1	SW480	log$D_{7.4}$	log$D_{7.4}$[a]
1	196 ± 27	7.5 ± 1.2	39 ± 3	–2.04 ± 0.08	
2	>320	12 ± 2	47 ± 3	–1.63 ± 0.08	–1.47 ± 0.11
3	>320	27 ± 3	53 ± 2	–1.13 ± 0.02	–1.31 ± 0.07
4	>320	20 ± 3	54 ± 10	–1.55 ± 0.08	
5	108 ± 5	13 ± 1	20 ± 3	–1.43 ± 0.08	

6	>320	13 ± 2	63 ± 10	–1.77 ± 0.12	
7	>320	23 ± 2	71 ± 15	–1.75 ± 0.02	
8	>320	17 ± 3	38 ± 12	–1.16 ± 0.02	
1*[b]	629 ± 13	89 ± 11	140 ± 36		
4*[b]	>320	114 ± 37	237 ± 47		
5*[b]	>640	148 ± 38	274 ± 40		

[a] in the presence of 0.1 M KCl; [b] data taken from ref. 13.

Conclusions

Reactions of potential anticancer drugs with amino acids have been studied by different groups,[32,43,44] but mainly in solution by ^{1}H NMR spectroscopy without isolation of the resulting products. We have succeeded to prepare a series of ruthenium-nitrosyl complexes with amino acids of the general formula (*n*Bu$_4$N)[RuCl$_3$(AA–H)(NO)], where AA = Gly, L-Ala, L-Val, L-Pro, D-Pro, L-Ser, L-Thr and L-Tyr, in addition to two complexes documented in the literature with L-His and L-Met, namely [RuCl$_2$(L-His)(NO)],[10] and [RuCl$_2$(L-Met)(NO)].[11] X-ray crystallographic studies have shown that in crystal structures of **1**–**8**, like in the previously reported osmium counterparts (*n*Bu$_4$N)[OsCl$_3$(AA–H)(NO)],[13] where AA = Gly, L-Pro and D-Pro, the carboxylate oxygen is a more preferred ligand in *trans* position to the coordinated nitrosyl ligand than the chloride ligand, secondary or primary amine. Likewise, the only isomer isolated from reactions of [RuCl$_5$(NO)]$^{2-}$ with eight amino acids is *mer*(Cl),*trans*(NO,O)-(*n*Bu$_4$N)[OsCl$_3$(AA–H)(NO)]. The results of the present study demonstrate that aminoacids used in this work are potential biological ligands for ruthenium-nitrosyl-based drug candidates in the blood serum and in the cytosol. A comparison with previously reported osmium analogues reveals a favorable influence of ruthenium on antiproliferative activity in human cancer cell lines *in vitro*, probably via hydrolysis pathways, although the cytotoxicity of ruthenium complexes with amino acids is either moderate or low depending on human cancer cell line. Whether this is a result of their low uptake into the cells taking into account their reduced lipophilicity or effective efflux as a part of detoxification mechanism, this should be clarified in ongoing research. Variation of the amino acid ligand has an even smaller impact on this activity within the range of

amino acids employed. Nevertheless, the synthesis of ruthenium- and osmium-nitrosyl complexes with other amino acids, and, in particular, Met, His and Cys, deserves attention as this will provide the opportunity to investigate their biological effects, which may differ from those studied in the present work. Collectively this may help in elucidating the mechanism of action of ruthenium and osmium-nitrosyl complexes with azole heterocycles. Activation of amino acidate ligands upon coordination to the metal may lead to specific intracellular chemistry and the resulting species may play a major role in either detoxification or therapeutic activity. According to other authors[45] oxidation of the sulfur atom of the tripeptide glutathione afforded sulfenato complexes, and binding to DNA mediated by these complexes may play a role in the mechanism of action of RM175. Similar behavior of coordinated cysteine has not been documented, but may be also envisaged.

Supporting Information

One-dimensional chains in a) **1**, b) **2** and c) **3** assembled via N−H···Cl hydrogen bonding (Figure S1), one-dimensional chains assembled via N−H···O hydrogen bonding in a) **4** and b) **5** (Figure S2), one-dimensional chains assembled via N−H···O and O−H···Cl hydrogen bonding in a) **6**, b) and c) **7** (two independent supramolecular chains) (Figure S3), one-dimensional supramolecular chains assembled via N−H···Cl and O−H···O hydrogen bonding in **8** (Figure S4), Cyclic voltammograms with several cycles of potential for **3**, **5**, **6** and **7** at 100 mV/s on glass carbon electrode (Figures S5−S8), hydrogen bonding parameters in **1**–**8** (Table S1), crystallographic data in CIF format. ^{1}H NMR and mass spectra of **1**, **4**, **5** and **8** are shown in Figures S9, S11S13 and log$D_{7.4}$ values of the complexes **1**–**8**.

AUTHOR INFORMATION

Corresponding Author

E-mail: dominique.luneau@univ-lyon1.fr (D.L.); vladimir.arion@univie.ac.at (V. B. A.)

Notes

The authors declare no competing financial interest.

ACKNOWLEDGMENTS

We thank Alexander Roller for collection of X-ray data and Ricarda Bugl for support in acquisition of the mass spectra. We are also indebted to the Austrian Science Fund (FWF) and the Agence Nationale de Recherche (France) for financial support of the bilateral project I374-N19 and ANR-09-BLAN-0420-01 (VILYGRu), respectively. The PHC Amadeus and OEAD (project no FR01/2012), as well as the Hungarian Research Foundation OTKA 103905 are also acknowledged for their support.

REFERENCES

(1) (a) Richter-Addo, G. B.; Legdzins, P. *Metal Nitrosyls*; Oxford: New York, 1992. (b) Rosen, G. M.; Tsai, P.; Pou, S. *Chem. Rev.* **2002**, *102*, 1191−1199. (c) Wasser, I. M.; De Vries, S.; Moënne-Loccoz, P.; Schröder, I.; Karlin, K. D. *Chem. Rev.* **2002**, *102*, 1201−1234.

(2) Fukumura, D.; Kashiwagi, S.; Jain, R. K. *Nat. Rev. Cancer* **2006**, *6*, 521−534.

(3) (a) Rademaker-Lakhai, J. M.; Van den Bongard, S.; Pluim, D.; Beijnen, J. H.; Schellens, J. H. M. *Clin. Cancer Res*. **2004**, *10*, 3717−3727. (b) Alessio, E.; Mestroni, G.; Bergamo, B.; Sava, G. *Curr. Top. Med. Chem.* **2004**, *4*, 1525−1535.

(4) Morbidelli, L.; Donnini, S.; Filipi, S.; Messori, L.; Picciolo, F.; Sava, G.; Ziche, M. *Br. J. Cancer* **2003**, *88*, 1484−1491.

(5) Jørgensen, C.K., *Coord. Chem. Rev.* **1966**, *1*, 164−178.

(6) Hirano, T.; Oi, T.; Nagao, H.; Morokuma, K. *Inorg. Chem*. **2003**, *42*, 6575−6583.

(7) (a) Coppens, P.; Novozhilova, I.; Kovalevsky, A., *Chem. Rev.* **2002**, *102*, 861−883. (b) Zangl, A.; Klüfers, P.; Schaniel, D.; Woike, Th. *Dalton Trans.* **2009**, 1034−1045.

(8) Ishiyama T.; Matsumura T. *Bull. Chem. Soc. Jpn.,* **1979**, *52*, 619−620.

(9) Ishiyama T.; Matsumura T. *Annual Report of the Radiation Center of Osaka Prefecture*, **1980**, *21*, 7–9.

(10) Zangl, A.; Klüfers, P.; Schaniel D.; Woike, T. *Dalton Trans.* **2009**, 1034–1045.

(11) Balakaeva, T. A.; Churakov, A. V.; Ezernitskaya, M. G.; Kuz'mina, L. G.; Lokshin, B. V.; Efimenko, I. A. *Koord. Khim.* **1999**, *25*, 621−625.

(12) Hirano, T.; Oi, T.; Nagao, H.; Morokuma, K. *Inorg. Chem*. **2003**, *42*, 6575−6583.

(13) Gavriluta, A.; Novak, M.; Tommasino, J. B.; Meier, S. M.; Jakupec, M. A.; Luneau, D.; Arion, V. B. *Z. Anorg. Allg. Chem.* **2013**, *639*, 1590–1597.
(14) Gavriluta, A.; Büchel, G. E.; Freitag, L.; Novitchi, G.; Tommasino, J. B.; Jeanneau, E.; Kuhn, P.-S.; González, L.; Arion, V. B.; Luneau, D. *Inorg. Chem.* **2013**, *52*, 6260–6272.
(15) Büchel, G. E.; Gavriluta, A.; Novak, M.; Meier, S.; Jakupec, M. A.; Cuzan, O.; Turta, C.; Tommasino, J.-B.; Jeanneau, E.; Novitchi, G.; Luneau, D.; Arion, V. B. *Inorg. Chem.* **2013**, *52*, 6273–6285.
(16) Peacock, A. F. A.; Melchart, M.; Deeth, R.; Habtemariam, A.; Parsons, S.; Sadler, P. J. *Chem. Eur. J.* **2007**, *13*, 2601–2613.
(17) Peacock, A. F. A.; Habtemariam, A.; Moggach, S. A.; Prescimone, A.; Parsons, S.; Sadler, P. J. *Inorg. Chem.* **2007**, *46*, 4049–4059.
(18) Cebrián-Losantos, B.; Krokhin, A. A.; Stepanenko, I. N.; Eichinger, R.; Jakupec, M. A.; Arion, V. B.; Keppler, B. K. *Inorg. Chem.* **2007**, *46*, 5023–5033.
(19) Stepanenko, I. N.; Krokhin, A. A.; John, R. O.; Roller, A.; Arion, V. B.; Jakupec, M. A.; Keppler, B. K. *Inorg. Chem.* **2008**, *47*, 7338–7347.
(20) Büchel, G. E.; Stepanenko, I. N.; Hejl, M.; Jakupec, M. A.; Arion, V. B.; Keppler, B. K. *Inorg. Chem.* **2009**, *48*, 10737–10747.
(21) Honn, K. V.; Singley, J. A.; Chavin, W. *Proc. Soc. Exp. Biol. Med.* **1975**, *149*, 344–347.
(22) (a) Paul, L. E. H.; Furrer, J.; Therrien, B. *J. Organomet. Chem.* **2013**, 734, 45–52. (b) Santini, C.; Pellei, M.; Gandin, V.; Porchia, M.; Tisato, F.; Marzano, C. *Chem. Rev.* DOI: 10.1021/cr400135x.
(23) (a) Alden, W. W.; Repta, A. J. *Chem.-Biol. Interact.* **1984**, *48*, 121–124. (b) Melvic, J. E.; Petersen, O. E. *Inorg. Chim. Acta* **1987**, *137*, 115–118.
(24) Bučinský, L.; Büchel, G. E.; Ponec, R.; Rapta, P.; Breza, M.; Kožíšek, J.; Gall, M.; Biskupič, S.; Fronc, M.; Schiessl, K.; Cuzan, O.; Prodius, D.; Turta, C.; Shova, S.; Zając, D. A.; Arion, V.B. *Eur. J. Inorg. Chem.* **2013**, 2505–2519.
(25) Enyedy, E.; Hollender, D.; Kiss, T. *J. Pharm. Biomed. Anal*. **2011**, *54*, 1073–1081.
(26) *SAINT-Plus*, version 7.06a and APEX2; Bruker-Nonius AXS Inc.: Madison, WI, **2004**.

(27) Sheldrick, G. M. *Acta Crystallogr.* **2008**, *A64*, 112–122.

(28) Burnett, M.N.; Johnson, G. K. ORTEPIII. Report ORNL-6895. OAK Ridge National Laboratory; Tennessee, **1996**.

(29) Reedijk, J., *Chem. Rev.* **1999**, *99*, 2499–2510.

(30) Reedijk, J., *Proc. Natl. Acad. Sci. USA*, **2003**, *100*, 3611–3616.

(31) Chen, Y.; Guo, Z. J.; Murdoch, P. D.; Zang, E. L.; Sadler, P. J. *J. Chem Soc. Dalton Trans.* **1998**, 1503–1508.

(32) Wang, F.; Chen, H.; Parkinson, J. A.; del S. Murdoch, P.; Sadler, P. J. *Inorg. Chem.* **2002**, *41*, 4509–4523.

(33) Wang, F.; Bella, J.; Parkinson, J. A, Sadler, P. J. *J. Biol. Inorg. Chem.* **2005**, *10*, 147–155.

(34) Yan, Y. K.; Melchart, M.; Habtemariam, A.; Sadler, P. J. *Chem. Commun.* **2005**, 4764–4776.

(35) Aird, R. E.; Cummings, J.; Ritchie, A. A.; Muir, M.; Morris, R. E.; Chen, H.; Sadler, P. J.; Jodrell, D. I. *Br. J. Cancer* **2002**, *86*, l652–1657.

(36) Paul, L. E. H.; Therrien, B.; Furrer, J. *Inorg. Chem.* **2012**, *51*, 1057–1067.

(37) Severin, K.; Bergs, R.; Beck, W. *Angew. Chem. Int. Ed. Engl.* **1998**, *37*, 1634–1654.

(38) Frausin, F.; Cochietto, M.; Bergamo, A.; Scarcia, V.; Furlani, A.; Sava, J. *Cancer Chemother. Pharmacol.* **2002**, *50*, 405–411.

(39) (a) Keniley, L. K., Jr., Dupont, N.; Ray, L.; Ding, J.; Kovnir, K.; Hoyt, J. M.; Hauser, A.; Shatruk, M. *Inorg Chem.* **2013,** *52*, 8040−8052. (b) Zhang, Y.-M.; Wu, S.-H.; Yao, C.-J.; Nie, H.-J.; Zhong, Y.-W. *Inorg. Chem.* **2012**, *51*, 11387−11395. (c) Lever, A. B. P. *Inorg. Chem.* **1990**, *29*, 1271–1285.

(40) (a) Marangoni, D. G.; Wylie, I. G. N.; Roscoe, S. G. *Bioelectrochem. Bioenerg.* **1991**, *25*, 269–284. (b) Marangoni, D. G.; Smith, R. S.; Roscoe, S. G. *Can. J. Chem*. **1989**, *67*, 921–926. (c) Malfoy, B.; Reynaud, J. A. *J. Electroanal. Chem*. **1980**, *114*, 213–223.

(41) (a) Tsierkezos, N. G. *J. Sol. Chem.* **2007**, *36*, 289–302; (b) Bond, A. M.; Oldham, K. B.; Snook, G. H. *Anal. Chem.* **2000**, *72*, 3492–3496.

(42) Pombeiro, A. J. L.; Guedes da Silva, M. F. C.; Lemos, M. A. N. D. A. *Coord. Chem. Rev.* **2001**, *219-221*, 53–80.

(43) Kurzwernhart, A.; Kandioller, W.; Enyedy, É. A.; Novak, M.; Jakupec, M. A.; Keppler, B. K.; Hartinger, C. G. *Dalton Trans.* **2013**, *42*, 6193–6202.

(44) Egbewande, F. A.; Paul, L. E. H.; Therrien, B.; Furrer, J. *Eur. J. Inorg. Chem.* DOI:10.1002/ejic.201301297.

(45) Wang, F.; Xu, J.; Habtemariam, A.; Bella, J.; Sadler, P. J. *J. Am. Chem. Soc.* **2005**, *127*, 17734–17743.

For Table of Contents only